The expression of virulence by the *Cryptococcus neoformans* VNIa-5 lineage is plastic and associated with host immune background.

Trieu Phan Hai[1], Thanh Lam Tuan[1], Duong Van Anh[1], Trinh Nguyen Mai[1], Lan Nguyen Phu Huong[2], Guy E Thwaites[1, 3], Errin Johnson[4], Nguyen Van Vinh Chau[2], Phil Ashton[1, 3], Jeremy Day[1, 3]

1. Oxford University Clinical Research Unit, Wellcome Trust Asia Africa Programme, 764 Vo Van Kiet, Quan 5, Ho Chi Minh City, Vietnam

2. Hospital for Tropical Diseases, 764 Vo Van Kiet, Ho Chi Minh City, Viet Nam

3. Nuffield Department of Clinical Medicine, University of Oxford, Old Road Campus, Headington, Oxford OX3 7BN UK

4. Sir William Dunn School of Pathology, University of Oxford, S Parks Rd, Oxford OX1 3RE, United Kingdom UK

Corresponding author:

J N Day

Oxford University CLinincal Research Unit

764 Vo Van Kiet

Quan 5

Ho Chi Minh City

Vietnam

Email:jday@oucru.org

Key words:

Cryptococcus neoformans; Meningitis; Immunocompetent; HIV; Virulence; Pathogenesis

Abstract

Cryptococcus neoformans most frequently causes disease in immunocompetent patients. However, in Vietnam and east Asia, disease is frequently reported in apparently immunocompetent patients. We have previously shown that almost all such disease is due to a specific lineage of C. neoformans – VNIa-5. However, in HIV infected patients, infections due to this lineage are not associated with worse outcomes. Here, we demonstrate that the VNIa-5 presents different virulence phenotypes depending on its source. Isolates derived from immunocompetent patients are more virulent than those from HIV infected patients or the environment. Moreover, the virulence phenotype is plastic – sterile culture filtrate from highly virulent VNIa-5 strains can induce increased virulence in less virulent VNIa-5 isolates, which in turn can then induce increased virulence in their low virulence states. We present evidence that this phenomenon is driven by secreted proteins associated with extra-cellular vesicles.

Introduction

Cryptococcal meningitis is a devastating disease due to infection with encapsulated yeasts of the *Cryptococcus* genus. Seven species (*Cryptococcus neoformans*, *C. deneoformans*, *C. gattii*, *C. bacillisporus*, *C. deuterogattii*, *C. tetragattii*, *C. decagattii*) are well recognised to cause human disease[1]. Disease most frequently occurs in immunosuppressed patients, but the *Cryptococcus gattii* species complex has been frequently associated with disease in immunocompetent patients[2]. The *C. gattii* species complex is limited to areas of tropical and sub-tropical/temperate rainforest[3].

The vast majority of human cryptococcal meningitis occurs in HIV infected patients and is due to *Cryptococcus neoformans*. There are an estimated 223,000 cases per year resulting in 181, 000 deaths[4]. Disease in HIV infected patients has been driven by the clonal expansion of a small number of well-defined lineages of *C. neoformans*, and while these are widely dispersed globally, in most countries a single lineage predominates[5]. Vietnam is unusual in having two co-dominant lineages circulating– VNIa-5 and VNIa-4 – with each accounting for about 35-40% of cases of meningitis in HIV infected patients[5-7].

In addition to HIV-associated disease, cryptococcal meningitis is also well-described in HIV uninfected patients in southeast and east Asia[8-12]. Such patients account for about 20% of cases at our hospital in Vietnam[12]. The majority of patients are apparently immunocompetent, with no other evidence to suggest underlying immune deficit. Outcomes are similar to those seen in HIV patients, with 3 month mortality rates in the order of 20-30%[12]. Contrary to expectation, most infections in these patients (80%) are due to *C. neoformans*, rather than *C. gattii*[13]. We have previously identified a strong association between the *C. neoformans* VNIa-5 lineage and disease in these apparently immunocompetent patients – it accounts for approximatley 90% of cases due to *C. neoformans*[5,6,13]. Furthermore, HIV uninfected patients with cryptococcal meningitis due to other lineages are statistically significantly more likely to have co-morbidities associated with immune compromise[13]. This suggests that isolates of the VNIa-5 lineage have increased pathogenic potential. Of note, we do not observe clustering of isolates within the VNIa-5 lineage according to host immune phenotype, suggesting that the entire lineage has the potential to cause disease in immunocompetent people[5]. Despite this apparent increase in pathogenic potential, in HIV infected patients meningitis due to the VNIa-5 lineage does not have worse outcomes than that due to other lineages circulating in Vietnam – in other

words the lineage does not appear more virulent in HIV infected patients[6]. This could have one of two explanations. First, the VNIa-5 lineage is more pathogenic than other lineages and capable of causing disease in immunocompetent people. Alternatively, the lineage may be exploiting some undefined, VNIa-5 specific, defect in host immunity in HIV uninfected patients that enables infection and/or subsequent development of disease. Here, we demonstrate that, using the *Galleria mellonella* model of infection, we can detect differences in virulence between isolates of the VNIa-5 lineage of different ecological backgrounds. The most virulent isolates are isolates of the VNIa-5 lineage from HIV uninfected patients. Sterile culture filtrate from these highly virulent isolates can induce increased virulence in low virulence isolates of the same lineage from HIV patients or the environment. Such induced isolates can subsequently upregulate the virulence of other low virulence isolates, and their own 'naïve' self. This process is lineage specific and mediated through secreted proteins associated with extracellular vesicles.

Results

1. VNIa-5 isolates from immunocompetent patients are more virulent than VNIa-4 clinical isolates, and than VNIa-5 isolates from HIV infected patients or the environment.

We used the *Galleria* model of infection to compare the relative virulence of VNIa-5 isolates from different sources, and with clinical isolates of the VNIa-4 lineage. Details of the strains used are given in **Table 1 of the Supplementary Appendix**. First we compared 20 clinical isolates of VNIa-5 from HIV uninfected patients with 20 isolates of the VNIa-4 lineage from HIV infected patients. The Kaplan-Meier curves are shown in **Figure 1A**. There was a

significantly increased hazard of death in *Galleria* infected with VNIa-5 compared with VNIa-4 (Hazard Ratio (HR) 1.4, 95% Confidence Interval (95CI) 1.2-1.6, P<0.001). Because we had previously failed to identify worse survival in Vietnamese HIV infected patients with VNIa-5 infections, we next compared the relative virulence of VNIa-5 isolates according to their source – i.e whether they were derived from HIV uninfected apparently immunocompetent patients, HIV infected patients, or the environment. We found divergence of *Galleria* survival curves by this factor: infection with isolates from immunocompetent patients was associated with a significantly increased hazard of death compared with infection with isolates from HIV infected patients (HR 1.7, 95CI 1.3 – 2.4, P<0.001) or with isolates from the environment (HR 5.7, 95CI 3.9 – 8.4, P<0.001, **see figure 1B**). We repeatedly passaged(six-fold) environmental strains through *Galleria* hypothesising that the difference in virulence phenotype by ecological background was a function of a previous infection experience. However, the virulence phenotype of the environmental isolates remained stable over multiple passages through the *Galleria* model, with no change in the hazard of death between the infection with the 'naïve' environmental isolate versus infection with that isolate following six-times passage through the model (see **Supplementary Figure 1**).

2. VNIa-5 isolates from HIV uninfected patients express greater *in vitro* growth and thinner capsules than VNIa-5 isolates from HIV infected patients

We next compared the expression of *in vitro* phenotypic characteristics associated with virulence by VNIa-5 isolates depending on their source – i.e. whether they were from immunocompetent patients or from HIV infected patients. We compared 15 isolates from apparently immunocompetent patients with 15 isolates derived from HIV infected patients.

We tested growth rates at 30 and 37°C in YPD broth and in pooled human CSF, capsule size, extracellular urease and phospholipase production, and melanin production. Isolates from from HIV uninfected patients had moderate but statistically increased growth by 48 hours at 30°C and 37°C compared with isolates from HIV infected patients (median $4.5X10^5$ CFU/ml (Interqartile Range (IQR) $3.6\ X10^5$ - $5.2\ X10^5$) and $4\ X10^5$ CFU/ml (IQR $2.6\ X10^5$ - $5\ X10^5$) for immunocompetent isolates versus $3.3\ X10^5$ CFU/ml ($2.9\ X10^5$ - $4.5\ X10^5$) and $2.8\ X10^5$ CFU/ml ($2.2\ X10^5$ - $3.8\ X10^5$) for HIV derived isolates, P=0.004 and 0.002 respectively). There was no statistically significant difference in the ability of immunocompetent patient derived isolates to grow at 37°C (P=0.058) compared with 30°C; however, isolates from HIV infected patients appeared to have decreased growth at 37°C (P = 0.044). (see **Figure 2A**).

In contrast, isolates derived from immunocompetent patients appeared to have slower growth in *ex vivo* CSF compared with isolates derived from HIV infected patients, with median fungal burdens after 48 hours of $7X10^3$ CFU/ml (IQR$4.9\ X10^3$ - $1.0X10^4$) versus $1.9X10^4$ (IQR $6X10^3$ - $2.6X10^4$), P=0.02 (**Figure 2B**). They also expressed significantly thinner capsules (median thickness 1.3 microns, IQR 0.8 - 1.6) compared with isolates from HIV infected patients (median 1.5 microns, IQR 1.3 – 1.95), P<0.001, see **Figure 2D**. There was no difference in yeast cell diameter (median 3.45 micron vs 3.3 micron, P = 0.5, immunocompetent derived versus HIV derived isolates). All strains produced melanised colonies on L-DOPA agar and were urease positive. There was no difference in phospholipase production (data not shown).

3. Growth in sterile culture filtrate from VNIa-5 isolates from HIV uninfected patients, but not from HIV patients, induces increased virulence in HIV-associated and environmental VNIa-5 isolates of *C. neoformans*

We hypothesised that the increased virulence in *Galleria* seen in isolates derived from HIV uninfected patients is associated with their ability to cause disease in immunocompetent people. Isolates from HIV uninfected patients are distributed throughout the VNIa-5 lineage; presumably all isolates of the lineage should be capable of being in this state, and able to cause disease in immunocompetent hosts. We hypothesized that the development and/or maintenance of an increased virulence state is driven by inter-yeast communication. To test this we grew a low virulence environmental VNIa-5 isolate in culture medium supplemented with sterile culture filtrate from high virulence VNIa-5 isolates from immunocompetent patients, and then compared the virulence phenotypes of the isolates in *Galleria*. Growth in media supplemented with sterile culture filtrate from all 4 strains from immunocompetent patients resulted in increases in the virulence of the environmental isolates compared with its 'naïve' self, with the hazard of death with infection of the induced isolate increasing between 2.2 and 2.5 fold (**see Figure 3**). The change in virulence phenotype of the environmental isolates was stable over multiple generations and *Galleria* infection cycles (**see Supplementary Figure 2**).

In contrast, growth in media supplemented with pooled sterile culture filtrate from HIV-associated VNIa-5 isolates had no effect on the virulence phenotype of environmental isolates, **see Figure 4A** (HR1.4, 95CI 0.8-2.3, P=0.2, 'induced' isolate versus naïve isolate).

We next repeated the experiments but growing the environmental VNIa-5 isolate in medium supplemented with sterile culture filtrate from VNIa-4 isolates (necessarily derived

from HIV infected patients). This did not result in any significant change in the virulence of the environmental isolate (see **Figure 4B**). Similarly, growth in sterile culture filtrate derived from the *C. neoformans* H99 type-strain had no effect on virulence phenotype (see **Figure 4C**). Growing the VNIa-5 environmental isolate in medium supplemented with its own sterile culture filtrate from previous culture had no effect on virulence phenotype **Figure 4D**.

4. Culture filtrate from an induced VNIa-5 isolate will itself induce increased virulence in its naïve isogenic self

We then tested the effect of growing a 'naïve' low virulence VNIa-5 environmental isolate (LD2) in media supplemented with sterile culture filtrate from its previously 'induced' higher virulence self. First, we cultured the naïve LD2 isolate in culture medium supplemented with sterile culture filtrate from the highly virulent, immunocompetent derived isolate BMD761 for 48 hours. We harvested the cultured yeast cells by centrifugation and washing and purified them for single colony growth on solid agar. We termed this isolated 'iLD2'. We recultured iLD2 in liquid medium for 48 hours and harvested culture filtrate. We then recultured the naïve LD2 strain in medium supplemented with the sterile culture filtrate from iLD2 for 48 hours. We termed the resulting isolate 'iLD2-induced LD2' . We then compared the virulence phenotypes of the isolates from each experiment in the *Galleria* model – i.e. 'LD2', 'iLD2', 'iLD2-induced LD2' and BMD761. (see **figure 5**). We found that, like the sterile culture filtrate fromBMD761, the sterile culture filtrate of iLD2 was itself able to induce an increased state of virulence in its naïve self (nLD2).

187 **5. Virulence induction is associated with increased *ex vivo* CSF survival, higher fungal**
188 **burdens in *Galleria*, and reduced capsule size.**

189 We assessed the effect of culture filtrate induction on virulence-associated phenotypes
190 (thermotolerance, melanin formation, *ex vivo* CSF survival, fungal burden in *Galleria* and
191 capsule size ex-*Galleria*) by comparing the environmental LD2 before (naïve) and after its
192 induction (induced). There were no changes in thermotolerance (ability to grow *in vitro* at
193 30°C or 37°C) or in apparent melanization. However, the induced LD2 had superior growth
194 in *ex vivo* CSF compared with its naïve self, with higher fungal burdens after 48 hours
195 incubation (median 5.9 $X10^4$ CFU/ml, IQR 3.6$X10^4$ – 7.6$X10^4$ vs 3.5 $X10^4$ CFU/ml, IQR 2.3 –
196 5.7 $X10^4$, P= 0.02, see **Supplementary Figure 3a)**. Similarly, the 48 hour fungal burden in
197 *Galleria* hemolymph infected with the induced isolate was significantly higher than that of
198 its naïve self (median fungal burden 9.6 $X10^6$ CFU/g body weight (inter-quartile range 6.9
199 $X10^6$ - 1.4$X10^7$) versus 5.3 $X10^6$ CFU/g body weight (IQR 4.0 $X10^6$ - 6.7 $X10^6$, P=0.025), see
200 **Supplementary Figure 3b)**. However, induced LD2 isolates expressed significantly thinner
201 capsules compared with the naïve self both when grown *in vitro* (median capsule width 4.5
202 µm, IQR 3.3-6.4 versus 7.2 µm, IQR 4.5 – 9.8, P<0.001, induced versus naïve respectively) or
203 when recovered from larval hemolymph (P=0.03, see **Supplementary Figure 4)**. Both
204 induced LD2 and naïve LD2 had significantly thinner capsules than the highly virulent
205 immunocompetent associated strain BMD761 (P<0.001 and P=0.03 respectively).

206

207 **6. The inducing effect of sterile culture filtrate is abolished by boiling and protease,**
208 **but not freezing or nuclease treatment.**

We froze sterile culture filtrate from the hypervirulent strain BMD761 at -20^{o}C for 1 month. Upon thawing, its induction effect on the naïve environmental strain LD2 was maintained (**Figure 6A**). However, boiling sterile culture filtrate was associated with loss of induction effect (**Figure 6B**), as was treatment with Proteinase K (**Figure 6C**). However, incubation of sterile culture filtrate with RNase or DNase had no effect, and the induction property was conserved (**Figure 6D**).

7. The induction phenomenon is likely mediated via extracellular vesicles.

Extracellular vesicles (EVs) have been implicated in the pathogenic potential of *Cryptococcus neoformans* and the related organism *Cryptococcus gattii*. To gather circumstantial evidence to support this hypothesis, we added albumin, which disrupts EV function, to sterile culture filtrate and tested the effect on induction[14]. Adding bovine serum albumin to sterile culture filtrate resulted in a loss of the induction effect (see **Supplementary Figure 5**). We then used an ultracentrifugation-based extra-cellular vesicle separation protocol to produce an EV-free supernatant and EV-containing pellet fractions from sterile culture filtrate. Incubation of naïve LD2 in media supplemented with supernatant did not result in induction of increased virulence (**see Figure 7B and D**); conversely when we incubated naïve LD2 in media supplemented with the putatively EV containing pellet there was induction of increased virulence (**see Figure 7A and C**). Subsequent electron microscopy of ultracentrifugation pellets confirmed presence of EVs; EVs were not seen supernatant (**Figure 8**).

8. Induction is associated with increased expression of recognised virulence factor genes and increased expression of a number of hypothetical proteins

We next used RNA-seq to probe the transcriptional basis of the observed change in phenotype. RNA was extracted for six biological replicates and sequenced on an Illumina HiSeq 4000 for four samples; an environmental VNIa-5 (low virulence and termed naïve LD2 (nLD2)), a clinical VNIa-5 from an HIV uninfected patient (BMD761), environmental VNIa-5 in a state of increased virulence consequent to having been grown in media supplemented with sterile culture filtrate from clinical VNIa-5 (induced LD2: iLD2) and the naïve environmental VNIa-5 isolate (nLD2) grown in media supplemented with its own sterile culture filtrate from a previous culture of itself (self-induced LD2: siLD2). Between 6.4 and 12.2 million reads were mapped per replicate, and more than 97% of reads mapped to the H99 reference genome in each replicate (full details in **Supplementary Table 2**). The virulence phenotypes of the isolates from all experiments, along with the inducing/non-inducing effect of their associated sCFs were confirmed in all cases - i.e. that the isolates had the expected virulence in *Galleria*, and that their associated culture filtrate was inducing (BMD761, iLD2 and siLD2) or non-inducing (nLD2). We confirmed strain identities by identifying SNPs unique to each isolate from corresponding whole genome sequencing data, and checking for the presence of these SNPs in the RNA-seq data.

To get an overall representation of the similarity of the transcriptomes of the four samples, we performed a PCA analysis on read counts per gene (see **Supplementary Figure 6**). The majority of replicates clustered by their sample type. There were some outliers, three of the BMD761 replicates did not group with the primary cluster of three similar samples, although two of these replicates were more distant from the primary cluster in the second dimension

of the PCA, which only explained 18% of the variance. Two replicates of LD2 and one replicate of induced LD2 were also separated from the primary clusters of their sample types. Despite these outliers, a clear pattern can be discerned, with a different overall pattern of gene expression between BMD761 and nLD2. The overall transcriptional profile of iLD2 shifted much closer to BMD761. In order to check for effects of the presence of culture filtrate, as opposed to culture filtrate from a high virulence biotype, we also supplemented the culture media of naïve LD2 with culture filtrate of a previous batch of naïve LD2; this self-induced LD2 also differed in it's transcriptional profile from the naïve LD2, but in a distinct way from the iLD2, and did not converge with the expression profile of BMD761.

Next, we performed a differential gene expression analysis in order to identify genes that were significantly (Wald test, Benjamini-Hochberg adjusted P value <0.05, log2 fold change $\geq$1 and $\leq$-1) up and down regulated. We found that there were 784 differentially expressed genes between BMD761 and naïve LD2, but after induction, there were only 244 differentially expressed genes between BMD761 and induced-LD2 (Figure 9). This contrasts with the large number of differences between these 2 isolates and LD2 in the other states (naïve or self-induced), where we found there were >1500 DEGs (Figure 9). This pattern of similarity between BMD761 and induced-LD2 and difference between the aforementioned and naïve or self-induced LD2 was maintained, even when the outliers were included (**Supplementary Figure 7**).

We mined the genes which were upregulated in both BMD761 and induced LD2 compared with naïve LD2 for functional associations which could explain this phenotypic difference. We focussed on genes which have an experimentally validated link to virulence[15], finding

277 that there were 17 up-regulated virulence factors in both BMD761 and Induced LD2 relative
278 to naïve LD2 [Supplementary Table 3].

279

280 **9. Metagenomics**

281 One potential cause of the induction phenomenon could be horizontal gene transfer such as
282 infection due to a mycovirus. We used Taxonomer, a metagenomics-based pathogen
283 detection tool (http://taxonomer.com) to interrogate all unmapped DNA (from whole
284 genome sequencing) and RNA (from RNAseq) unique to BMD761 and induced LD2,
285 compared with naive LD2 and self induced LD2, in order to identify DNA or RNA signatures
286 suggestive of a mycovirus infection associated with induction. We did not find any
287 convincing evidence to support the mycovirus hypothesis – we found a small number of
288 reads consistent with DNA viruses; however, none were expressed in every replicate and
289 the read counts were low.

290

291 **Discussion**

292 A number of lineages of *Cryptococcus neoformans* cause meningitis in humans in Vietnam,
293 but the vast majority of cases are due to either VNIa-4 or VNIa-5[5]. We have previously
294 shown that the VNIa-5 lineage is strongly associated with disease in apparently
295 immunocompetent patients[5,6]. Both VNIa-5 and VNIa-4 frequently affect our (severely
296 immunosuppressed) HIV infected patients[5,6]. VNIa-4 rarely causes disease in HIV uninfected
297 patients, and when it does, the patients are significantly more likely to have underlying
298 diseases associated with immunosuppression. Despite this difference in ability to infect

hosts of different immune competencies, mortality rates are no different in HIV infected patients whether they are infected with VNIa-4 or VNIa-5[6].

Here, we have found that the VNIa-5 lineage displays significant variability in virulence phenotype in the *Galleria* model of infection, and that this is associated with the particular isolate's ecological background – isolates from immunocompetent patients are more virulent than those from HIV-infected individuals or those recovered from the environment. The VNIa-5 isolates derived from immunocompetent patients are also significantly more virulent than VNIa-4 isolates, necessarily derived from HIV infected patients.

The differences in virulence phenotype of the VNIa-5 isolates are not explained by a specific within-lineage substructure - virulent isolates from immunocompetent patients do not cluster within, but are distributed throughout, the VNIa-5 phylogeny[5]. This suggests that any isolate of the VNIa-5 lineage should have the capacity to express a highly virulent phenotype, and therefore infect immunocompetent patients. Consistent with this, we found that the VNIa-5 virulence phenotype is highly plastic – less virulent isolates, derived from the environment, can be induced into a more virulent state by growing them in culture media that has been supplemented with sterile culture filtrate from highly virulent isolates, derived from immunocompetent patients. While we found HIV derived VNIa-5 isolates were somewhat more virulent that the environment-derived isolates, their sterile culture filtrate lacked this capacity and could not induce increased virulence. The induction effect was also limited to sterile culture filtrate derived from the VNIa-5 lineage – sterile culture filtrate from the VNIa-4 lineage, or from the VNIb H99 type strain, did not have the induction property. Therefore, we hypothesize that the induction effect seen with culture filtrate from immunocompetent patient-derived VNIa-5, and the virulence plasticity of the lineage, are

intimately associated with the ability of the lineage to cause disease in the immunocompetent host.

We found the increased virulence of VNIa-5 derived from immunocompetent patients was associated with differences in *in vitro* virulence phenotypes compared with isolates from HIV-infected patients, although the relationship was not simple. Isolates from immunocompetent patients had faster rates of growth at 30 and 37^{o}C, but had slower growth in *ex vivo* cerebrospinal fluid and expressed thinner capsules. Induction of the higher virulence state in the environmental isolate LD2 was also associated with increased fungal burdens in *Galleria*, and expression of thinner capsules. However, the induced LD2 isolate grew more rapidly in *ex vivo* CSF compared with its naïve self. It is not clear why the changes in *in vitro* phenotypes on induction were not entirely consistent with our findings when comparing isolates by source. It may reflect the fact that these measures of virulence are largely validated in relation to the ability of a strain to cause disease in humans irrespective of immune background, i.e. including those with HIV infection. Or, it may be that the induction phenomenon we have identified here is only a part of the mechanism that is associated with disease in immunocompetent humans. However, our transcriptional data suggest thet the change in virulence we are measuring in *Galleria* is real, because i) it is associated with increased expression of a number of virulence associated genes and ii) we saw a significant and remarkable convergence in gene expression between the highly virulence BMD761 isolate and the induced environmental isolate LD2.

The induction phenomenon we see is robust and repeatable. We do not believe it is an artefact of 'carry-over' of virulent organism from the sCF donor isolate, because we used 0.45 micron filters, which should exclude any donor cells, and every culture filtrate is tested for sterility through culture. Furthermore, the induced state is stable following purification

by culture on solid media. We can be certain that the convergence of the transcriptomic data from BMD761 and iLD2 is not confounded by contamination because we identified SNPs unique to each isolate within the context of nearly 900 *C. neoformans* genomes[5], and verified the identity of the strains in the RNA-seq data using these markers. Similarly we also do not believe that the effect on virulence in *Galleria* is due to 'carryover' of some agent (eg extra-cellular vesicles) from the donor isolate sCF, because induced isolates retain their increased virulence following purification on solid media.

The induction effect appears to include a protein component, since the inducing effect of sCF is lost with both boiling and protease treatment. Our data also sugest that the effect is associated with extra-cellular vesicles – the addition of albumin, which disrupts *Cryptococcus* vesicles, to sCF inhibited virulence induction[16]. We used an ultracentrifugation protocol[14] to concentrate EVs and showed that the induction effect was maintained in the EV containing pellet, and lost in the EV-free supernatant. We confirmed the presence/absence of EVs in the pellet/supernatant with transmission electron microscopy. The populations and compositions of EVs secreted by eukaryotic cells are complex. In addition to proteins they can contain small nucleic acids[14]. While we found no effect of nuclease treatment on the property of sCF, it is possible that we may have missed an effect because any small nucleic acids may have been protected within vesicles.

A striking feature of the induction effect is the stability of the resulting phenotype, and the transmissibility of the phenomenon. One possible explanation is that the effect we are observing is an infection event by a mycovirus. To investigate this possibility we interrogated any unmapped reads from our whole genome and transcriptome sequence data using a metagenomic platform. We found no convincing evidence of viral infection. A further possibility is that the effect is prion mediated – an EV-associated prion (Sup35p) has

been implicated in cell-to-cell communication in *Saccharomyces cerevisiae*, although the effect is not well-conserved across species[17,18]. However, the effect we observed of sCF in our isolates was heat labile, suggesting a prion-driven mechanism is unlikely.

On balance, we believe the phenomenon we have described is most likely mediated through extra-cellular vesicles associated with one or more proteins. Small nucleic acids may be involved. Such an EV-dependent mechanism is plausible - their production has been demonstrated for a number of fungal pathogens, including *Cryptococcus*[19-23]. A specific role in the pathogenicity of *C.neoformans* was first postulated in 2008[22] - EVs have been shown to contain virulence-associated factors including capsular components and laccase[20]. In addition to proteins, EVs are also associated with small DNAs and RNAs which could influence virulence[14,23-25]. Recently, EVs have been shown to mediate virulence of an outbreak strain of the related species *C.gattii*[14]. The EV-mediated effect was dose-dependent, manifested as increased growth, and required both EV-associated protein and RNA, providing strong evidence of EV uptake enabling inter-yeast communication. The phenomenon differed from our observations in that it was seen in macrophage culture, and onward transmissibility of the phenotype was not reported.

Such inter-yeast signalling systems, associated specifically with changes in virulence, are exciting potential therapeutic targets. A great challenge in treating HIV uninfected patients with cryptococcal meningitis, is knowing when it is is safe to stop antifungal therapy, and in fact complete cure may take many months of treatment, or even life-long antifungal therapy. This contrasts with HIV infected patients, where there is a modifiable immune pathology, and once antiretroviral therapy has allowed immune recovery, as evidenced by peripheral blood CD4 counts, we know it is safe to stop antifungal treatment for most

patients. Disrupting inter-yeast signalling associated with control of virulence, alongside conventional treatment, might ultimately allow cure in immunocompetent patients. Where and when the induction phenomenon occurs in relation to human disease is unclear. It may be a rare event that occurs somewhere in the environment, perhaps as a result of interaction with other micro-organisms, or due to animal infection, or it might occur in humans themselves[26-29]. If the former, then we would on occasion expect to see such inducing isolates in HIV infected patients. We would need to characterise large numbers of isolates from HIV infected patients to explore this. While there are significant numbers of people living with HIV in southeast and east Asia, the HIV prevalence is relatively low. In Vietnam, it is estimated to be <1%[30]. Therefore, if the induction of virulence in VNIa-5 isolates occurs in the environment and is a rare event, we would indeed expect to see the majority of cases in immunocompetent patients rather than HIV patients, since immunocompetent patients so outnumber those with HIV infection.

Conclusion

The virulence phenotype of Cryptococcus neoformans VNIa-5 in the Galleria infection model is associated with the isolate source. Isolates from immunocompetent patients are the most virulent; those from the environment the least. Since highly virulent isolates do not cluster within the lineage, it is likely that all isolates have the capacity to cause disease in the immunocompetent, and indeed we found the virulence phenotype to be highly plastic. Regulation of virulence in part appears to be influenced by inter-yeast signalling through the secretion of proteins which our data suggest are associated with extracellular vesicles. The change in phenotype from ‘naïve’ to ‘induced’ is accompanied by transcriptional re-modelling and converged of the induced isolate with the ‘inducer’. Once an isolate of the

lineage has had its virulence induced, it can turn induce increased virulence in other VNIa-5 isolates. The induction phenomenon is VNIa-5 specific, and presumably is key in the lineages ability to cause disease in the immunocompetent. Better understanding the mechanism may reveal novel therapeutic targets.

Funding

Funded by a Wellcome Trust Intermediate Fellowship to JND Grant number: WT097147MA

Methods

Isolates

Clinical isolates were derived from Vietnamese patients with cryptococcal meningitis who had been enrolled into descriptive and randomised intervention studies performed by our institute in collaboration with the Hospital for Tropical Diseases, Ho Chi Minh City[12,31,32]. All isolates were from cerebrospinal fluid obtained at the point of diagnosis and/or study entry, and stored on Microbank beads at -80^{o}C prior to revival on Sabouraud dextrose agar. Informed consent was obtained from all participants; all studies received ethical approval through the Oxford Tropical Ethics Committee, The Hospital for Tropical Diseases, and The Ministry of Health of Vietnam. All isolates have been previously sequenced and the data are publically available[5]. Isolates of the lineage and human immune phenotype of interest (HIV infected or not) were randomly selected from the isolate database for subsequent experiments. Environmental isolates were obtained via randomised sampling of air, soil and tree bark in urban and rural areas within and around Ho Chi Minh City. All strains used were mating type alpha.

In vitro phenotyping

Temperature – dependent growth

Growth at high temperature and in *ex vivo* human CSF were tested as previously described with modifications for quantitative assessment[33]. *Cryptococcus spp* were cultured on Sabouraud agar for 2 days at 30°C. Inocula were made from single colonies and adjusted to 10^8 cells/ml, then serially 10-fold diluted and spotted in duplicate onto YPD agar in 5µl aliquots. Incubation was at 30°C or 37°C for 48 hours. After 48 hours, the number of colony forming units (CFU) was counted and expressed as CFU/ml.

Capsule production

Capusle thickness was assessed through growth on Dulbecco Modified Eagle Medium (DMEM) [supplemented with 4.5g/L glucose, L-glutamine, sodium pyruvate], $NaHCO_3$ 250mM, NaMOPS 1M, Neomycin 200mg/ml, Cefotaxime 100 mg/ml[34]. Plates were incubated at 37°C in 5 % CO_2 for 5 days. A suspension from a single colony was made in India ink visualized at 100X magnification using light microscopy (CX41, Olympus, Japan). Images were captured using a built-in DP71 camera (Olympus, Japan) and visualised using ImageJ (https://imagej.nih.gov/ij/index.html). Capsular thickness was calculated by subtracting yeast cell body diameter from the whole cell diameter. At least 30 individual microscopic yeast cells were assessed for each isolate.

462 **Melanization**

463 Melanin production was assessed by plating 5µl of 10^6cells/mL cell suspension onto L-DOPA
464 agar containing 1g/L L-asparagine , 1g/L glucose, 3g/L KH2PO4, 250mg/L MgSO4.7H2O,
465 1mg/L Thiamine HCl, 5µg/L Biotin, 100mg/L L-DOPA, 20g/L Bacto Agar (Fisher Scientific,
466 UK)[35,36]. Plates were incubated in the dark at 30°C. Differences in colony melanization were
467 compared visually with reference to H99 and an H99-derived mutant with diminished
468 melaninization in L-DOPA agar, kindly provided by the Perfect Lab, Duke University .

469

470 **Urease and phospholipase production**

471 Urease production was confirmed by spotting 5µl of 10^8cells/mL cell suspension onto
472 Christensen's agar with incubation at 30°C for 72 hours. *Cryptococcus neoformans* H99 type
473 strain and *Candida parapsilosis* ATCC 22019 were used as positive and negative controls.
474 Cultures were observed for the characteristic pink discoloration.

475 Extracellular phospholipase activity was confirmed on egg yolk medium as previously
476 described, with minor modifications again using a 5 µl aliquot of *C. neoformans* yeast
477 suspension (10^8 cells/ml) with incubation at 30°C for 72 hours[37]. The diameter of the
478 precipitation zone (D) formed around a colony in relation to the diameter of the respective
479 colony itself (d) was recorded for 5 selected colonies of each isolate (N=450 total) collected
480 after 72 hours incubation. The D/d ratio for each isolate was calculated. H99 was included
481 for reference in each experimental batch. The final result for each isolate was expressed as
482 the ratio D/d ratio. Type strain H99 was used as a quality control.

483

Survival in *ex vivo* cerebrospinal fluid

CSF was prepared by pooling and filtering (Millipore 0.45 micron membranes, Merck) CSF samples taken prior to antifungal therapy from HIV infected patients participating in clinical trials. CSf was stored at -80^{o}C prior to use. An inoculum of 10^{7} cells/mL of each isolate of interest was prepared using a Cellometer X2 (Nexcelom) cell counter. 10 uL of inoculum was added to 90 uL of CSF and PBS followed by incubation at 30^{o}C for 3 days. After 72 hours the resulting culture was serially tenfold diluted, spotted onto Sabouraud plates and incubated at 30^{o}C for 3 days for quantification. Tested trains were inoculated alongside H99 and the ΔENA1 negative control (which lacks a cation-ATPase-transporter resulting in decreased viability in human CSF and macrophages, strain provided by the Perfect Lab, Duke University)[33]. Two biological replicates were performed per isolate.

Galleria infection model

Late instar isogenic wild type *Galleria mellonella* larvae (30 days from oviposition of the adult moth) were sourced from U U Animal, (Ho Chi Minh city, Vietnam). All larvae were kept at 16^{o}C in bran in the dark. Larvae for experimentation were selected according to the following criteria: weight 250-300 mg, healthy colour (beige). Yeasts were revived from frozen stock (Microbank Beads) on SDA plates for 72 hours. Single colonies were picked and cultured in YPD broth for 24 to 48 hours in a shaking incubator (SI-300, Jeio Tech), at 150 rpm at 30^{o}C until the concentration of cells was as at least 10^{8} cells/mL. The pellet was collected with centrifuge at 8000 rpm in 1 minute and subsequently washed twice with PBS. The cell suspension was adjusted to a density of 10^{8} cells/mL using a Cellometer X2 (Nexcelom Bioscience, USA). Ten µL of inoculum (10^{6} cells/larva) were used for injection per

larva. All inocula were relabeled by an independent person such that the operator/assessor was blind to the nature of the inoculum used in each batch of larvae (i.e. the survival experiments were blinded). Larvae were inoculated through injection using a sterile Hamilton syringe into the most caudal left pro-leg. 15-20 larvae were infected per cryptococcal isolate. Each cryptococcal strain was injected into 15 or 20 larvae. Every survival experiment was internally contemporaneously controlled using larvae of the same batch, a negative control (PBS) (physical injury and sterility), and uninjected larvae and the 2 or more experimental arms of interest. Infected larvae were incubated at 37^{o}C for ten days and checked daily for mortality using physical stimulation with forceps.

Culture Filtrate preparation

All isolates were grown in 7.5 ml YPD broth at 30^{o}C with shaking for 48 hours followed by centrifugation at 8000 rpm for 1 minute. The resulting supernatant was filtered using a Millipore membrane filter 0.45 □m (Merck), and checked for sterility by plating onto Sabouraud's agar and into BHI broth with incubation at 30^{o}C for seven days.

Induction experiments

2.5 mls of the culture filtrate of interest was added to 5mls of sterile YPD broth (total volume 7.5mls). A single purified colony of the isolate of interest was added to the resulting culture medium and incubated for 48 hours with shaking at 30^{o}C. Cells were separated by centrifugation (1 minute at 8000 rpm), washed twice with PBS and pellet spread on Sabouraud agar plate for single colony purification. Single colony was then inoculated into YPD broth, and incubated with shaking for 48 hours for inoculum preparation.

530

531 **Confirmation of virulence phenotype stability in *Galleria***

532 Yeast was recovered from *Galleria* hemolymph, cultured for purity on SDA, recultured in
533 YPD and reinoculated into *Galleria* as described 6 fold. Similarly purified culture derived
534 from hemolymph was repeatedly subcultured on solid media, frozen on Microbank beads,
535 revived, and re-inoculated into the *Galleria* model.

536

537 **Quantification of fungal burden in larvae**

538 Larvae infected with the strains of interest (5 dead larvae/biological replicate) were
539 collected at the point of death and gently squeezed to obtain 1 gram of hemolymph and fat
540 body using a sterile knife. Glass beads (3mm) and 1 mL of sterile water were added for
541 homogenization at 30Hz for 10 minutes (TissueLyser II, Qiagen). Homogenates were diluted
542 with PBS and inoculated onto SAB plates and incubated for 3 days at 30oC. The number of
543 colonies were counted to calculate the CFU/gram/larvae.

544

545 **Capsule size measurement from *Galleria***

546 Following infection with 10^6 cells, larvae were sacrificed 48 hours post-infection and
547 hemolymph extracted as above. Hemolymph was stained with India ink to visualise capsule
548 using light microscopy (at 1000X magnification) using an Olympus DP71 digital camera
549 (Olympus, Japan) and the proprietary Image-J software.

550

551

552 **Treatment of culture filtrate with freezing, heat, protease, and nuclease**

553 To check the stability of culture filtrate exposed to prolonged frozen storage, the culture
554 filtrate of BMD761 was kept at -20 ^{o}C for 33 days. The filtrate was brought to room
555 temperature prior to induction experiments. To denature protein by heat, filtrate of
556 BMD761 was boiled at 97 ^{o}C for 2 minutes. To denature protein chemically, filtrate was
557 incubated with Proteinase K (Sigma-Aldrich, UK) at a concentration of 100 μg/mL in the
558 presence of 30 mM Tris.HCl (pH=8) and 5 mM $CaCl_2$ at 37 ^{o}C for 1.5 hours. To degrade DNA,
559 28 μL DNAse I (Ambion, ThermoFisher, UK) was added to 700 μL DNAse I buffer and 7 mL
560 filtrate for 1 hour at 37^{o}C. To remove RNA, 2.5 mL filtrate was incubated with 50 μL RNAse
561 cocktail of RNAse A and RNAse T1 (Ambion, ThermoFisher Scientific,UK) for 1 hour at 37^{o}C.

562

563 **Confirmation of digestion of protein and nucleic acid in filtrate**

564 Protein digestion was confirmed by running treated and untreated culture filtrate on
565 precast polyacrylamide gel 4-20 % (Mini-PROTEAN® TGX Stain-Free™ Precast Gels, BIO-RAD)
566 at 200V for 40 mins. Precision Plus Protein Dual Xtra Standards (BIO-RAD) were loaded
567 alongside samples, including a proteinase K treated ladder.

568 Samples treated with nuclease were confirmed by loading in agarose gel 1.5 % followed by
569 electrophoresis for 60 mins at 100V, with 100bp DNA ladder.

570

571 **Extracellular vesicle preparation**

572 Isolates for experimentation were grown to stationary phase in 500ml of YPD broth at 37^{o}C
573 with shaking for 48 hours prior to transfer to 200mL centrifugation vessels. These were spun

574 at 15,000g for 10 minutes at 4°C. Supernatant was decanted and centrifugation repeated for
575 a further 10 minutes, then filtered through 0.45um filter membranes. The filtrate was then
576 concentrated using Amicon 100kDa ultrafiltration columns with centrifugation at 5000g for
577 15 minutes at 4°C. The EV containing retentate, was then ultracentrifuged at 150,000g at
578 4°C for 1 hour to provide EV containing pellet and EV-free supernatant.

579

580 **Electron Microscopy**

581 Pellet and supernatant resulting from ultracentrifugation were fixed in 2%
582 Paraformaldehyde (PFA) in 0.1M sodium Phosphate buffer at room temperature for 30
583 minutes. Samples were transferred to the Electron Microscopy Facility at the Sir William
584 Dunn School of Pathology, University of Oxford, UK for Transmission Electron Microscopy.

585

586 **Preparation of inducing broth using ultracentrifugation product**

587 Inducing broth consisted of 50uL ultracentrifuged product (either pellet or supernatant
588 fraction) added to fresh sterile YPD to achieve a final volume of 7.5 mL. A 100uL volume was
589 taken for culture as a test of sterility. Naive strains (a single colony each) were then
590 inoculated into inducing broth and incubated for 48 hours with shaking at 30°C. Yeast were
591 harvested in the normal manner via centrifugation 8000 rpm and washed twice with PBS
592 prior to subculture on solid agar. Inoculum for larva infection (10^8 cells/mL) were prepared
593 in PBS using a Nexelom cell counter; 10 uL (10^6 cells) were injected into the larvae.
594 Inoculum densities were checked through serial dilution and culture.

595

596 **RNAseq**

597 Three replicates of each strain were cultured in YPD broth for 96 hours at 30°C to determine
598 log phase for RNA extraction. An inoculum of 10^6 cells was grown in 7.5 mL of YPD broth by
599 agitating (200 rpm). At interval time point post-inoculation (0, 6, 20, 24, 30, 44, 54, 68, 72
600 and 96 hours), an aliquot of 50 uL was taken for quantification by plating in Sabouraud agar
601 plates. These plates were exposed to incubation at 30°C for 48 hours. Growth curves were
602 plotted using ggplot package and R version 3.4.0 software (R Foundation for Statistical
603 Computing, Vienna, Austria). Growth rates were determined using the formula growth
604 rate=$(\log10N_t\text{-}\log10N_o)*2.303/t\text{-}t_o$, where N indicates cell concentration at a particular time
605 point; and t indicates the time point).

606 For transcriptional experiments, single colonies of each isolate of interest were revived from
607 beads (Microbank, UK) stored at -80°C. Revived isolates (approximately 10^6 cells, counted
608 using a Cellometer) were grown in 7.5 ml of YPD broth by agitating for 18 hours at 30°C to
609 reach mid-log phase. RNA was harvested using the RiboPure™-Yeast RNA Isolation Kit
610 (Ambion, USA) according to the manufacturer's instructions. Extracted RNA samples were
611 subjected to quality control using an Agilent 2100 Bioanalyzer (Agilent, USA). The integrity
612 of total RNA was estimated using the RIN (RNA Integrity Number), which ranges from 1 to
613 10, with 1 being the most degraded. Samples with RIN greater than 7 qualified for RNA-Seq.
614 6 biological replicates were prepared of every experimental condition. RNA was eluted in
615 isopropanol and shipped at room temperature to Macrogen (Seoul, Korea) for library
616 preparation and sequencing.

617 Paired-end RNA-Seq libraries were constructed using the TruSeq stranded mRNA
618 preparation kit (Illumina, USA). Resulting cDNAs were ligated with sequencing adaptors and

619 sequenced using the Illumina HiSeq 2000 platform, generating ~11.2 million reads of 150 bp
620 per sample, resulting in an estimated 177-fold coverage.

621

622 **RNA sequencing analysis**

623 Raw reads were checked for quality using FastQC
624 (https://www.bioinformatics.babraham.ac.uk/projects/fastqc/). Adapters were removed
625 using scythe (https://github.com/vsbuffalo/scythe). The resulting reads were then further
626 checked based on Phred score and read length in order to trim low quality regions using
627 Trimmomatic (http://www.usadellab.org/cms/?page=trimmomatic). Sequenced reads were
628 aligned with the *C. neoformans* var. *grubii* H99 reference genome using HISAT2
629 (https://ccb.jhu.edu/software/hisat2/index.shtml). SAM (Sequences Alignment Map) files,
630 output of read alignment, were converted to BAM (Binary Alignment Map) files using
631 SAMtools (http://www.htslib.org). Finally featureCounts was used to count reads assigned
632 to genomic features (genes, exons, chromosome locations) on the reference genome[38]. The
633 output table of raw counts per gene for each sample was imported for gene expression
634 analysis using DESeq[39]. Library size differences were normalized internally[40].

635

636 **Metagenomic analysis**

637 Taxonomer, a metagenomics-based pathogen detection tool, was used to profile unmapped
638 mRNA expression reads and unmapped DNA from (previous) genome sequencing from the
639 Cryptococcus isolates. A web-based interface was used to visualize summary of taxonomic
640 composition and read abudance (available at http://taxonomer.com).

641

642 **Statistical data analysis**

643 Kaplan-Meyer survival curves were plotted using ggplot2 and survminer package (R version
644 3.4.2). The Log-rank test was used to compare differences in survival. Hazard Ratios were
645 estimated using the Cox proportional-hazards model. The Wilcoxon rank sum test was used
646 to compare fungal burdens between isolates. Capsule size was compared using the Kruskal-
647 Wallis test with P values adjusted for multiple comparisons with the Benjamini-Hochberg
648 method.

649

List of Figures

1. Figure 1

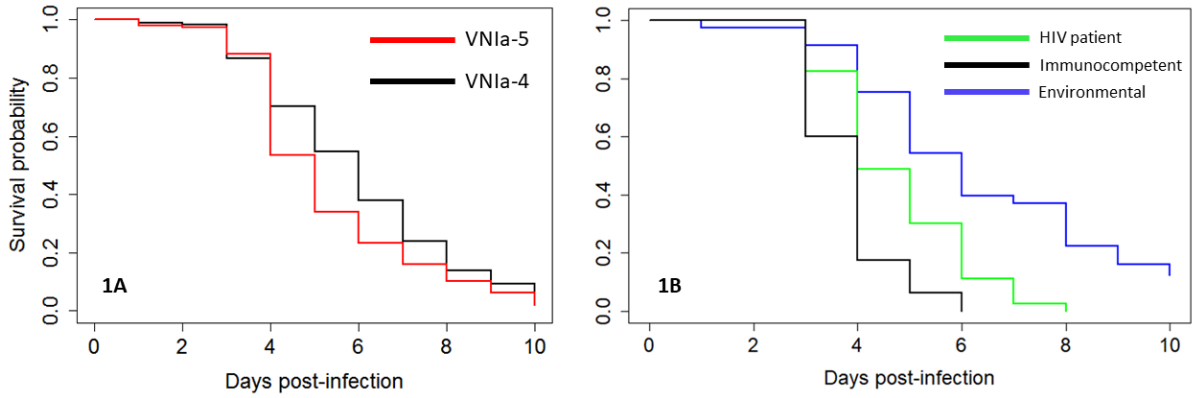

Figure 1A: Survival curves of *Galleria mellonella* infected with human cerebrospinal fluid derived isolates of *Cryptococcus neoformans* of lineage VNIa-5 (derived from immunocompetent patients) or lineage VNIa-4 (from HIV infected patients). N = 600 (20 isolates of each lineage, 15 larvae infected with each isolate, Hazard Ratio (95% Confidence interval): HR 1.4, 95CI 1.2,1.6; P<0.001 VNIa-5 versus VNIa-4).

Figure 1B: Survival curves of *G. mellonella* infected with *C. neoformans* lineage VNIa-5 isolates derived from immunocompetent patients (black line), HIV patients (green line), or the environment (blue line). 2 isolates of each source, 40 larvae per isolate. Hazard ratios and 95%CI for death: HIV derived vs environmental: 2.6, 95CI 1.8, 3.7; P< 0.001; immunocompetent derived versus environmental: 5.7; 95CI 3.9, 8.4; P< 0.001; Immunocompetent versus HIV derived: 1.7; 95CI 1.3 – 2.4, P<0.001. N=80 per arm.

2. Figure 2

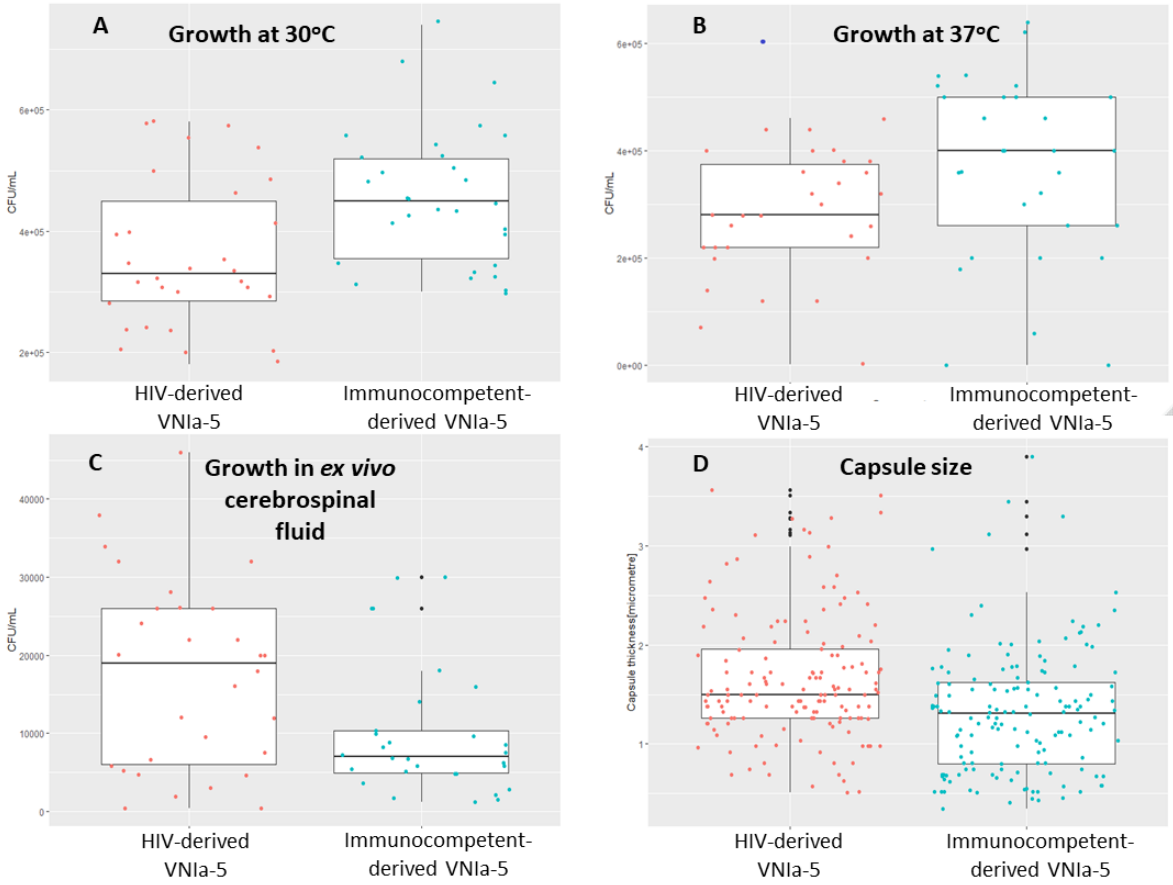

Figure 2: Comparative growth rates of VNIa-5 isolates in YNB broth at 30°C (panel A), 37°C (Panel B) an in *ex vivo* cerebrospinal fluid (C), and differences in capsule size (D) according to source – HIV infected patients or immunocompetent patients. There was statistically significant greater growth of isolates derived from immunocompetent patients at both temperatures (P=0.004 and P=0.002 for 30°C and 37°C respectively). There was reduced growth at 37°C for both sets of isolates, but this was only statistically significant for those derived from HIV infected patients. In contrast, isolates derived from immunocompetent patients appeared to have significantly impaired growth in *ex vivo* CSF compared with isolates from HIV infected patients (P=0.02). (Note that the Y-axis scales are not the same in each panel). For all experiments N=15 isolates of each type, with 2 biological replicates.

683 **3. Figure 3**

684

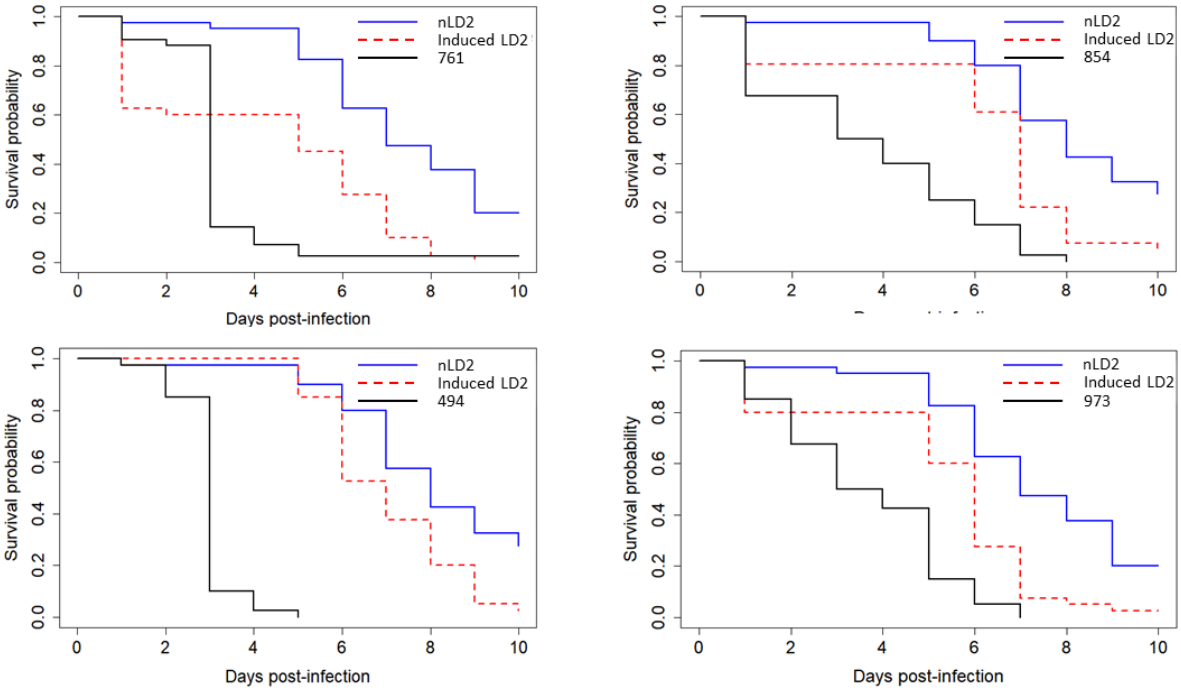

685

686

687 **Figure 3 : Survival curves for *G. mellonella* infected with 4 human isolates of *C. neoformans* lineage**

688 **VNIa-5 derived from HIV uninfected patients (BMD761, BMD854, BMD973 and BMD494), and**

689 **naïve environmental strain (nLD2) and nLD2 following growth in sterile culture filtrate from each**

690 **of the human derived isolates (induced LD2).** Hazard ratios of the risk of death, 95%CI and P values

691 for iLD2 versus nLD2 infections for each experiment are: HR 2.9, 95CI 1.8, 4.8 P<0.001; HR 2.5, 95CI

692 1.5, 4.0 P<0.001; HR 2.7, 95CI 1.7, 4.4 P<0.001 and HR 2.2, 95CI 1.4,3.6 P=0.001 respectively.

693

4. Figure 4

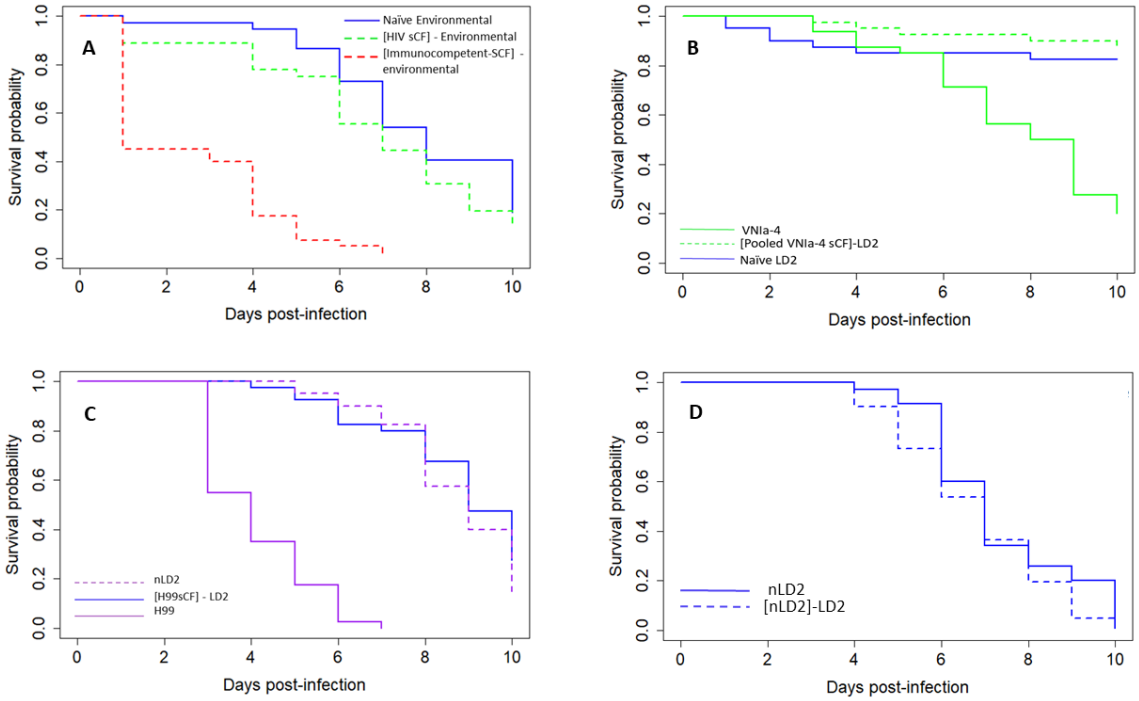

Figure 4: Survival curves of *Galleria* infected with naïve environmental isolate, or that environmental isolate following growth in media supplemented with sterile culture filtrate (sCF) of different sources, or the source of sCF. The square brackets refer to the source of the sCF.

Figure 4A: Survival curves for *G. mellonella* infected with environmental isolates of *C. neoformans* lineage VNIa-5 (naïve environmental, blue line), and infected with the same environmental isolates following their growth in media supplemented with pooled sterile culture filtrate from either VNIa-5 lineage isolates derived from HIV infected patients ([HIV-sCF], green dashed line) or from immunocompetent patients ([Immunocompetent-sCF], red dashed line). There is no significant increase in the hazard of death following infection with environmental isolates grown with sCF from HIV associated VNIa-5 isolates (HR 1.4 (95CI 0.8-2.3), P=0.2). Growth in media supplemented with sterile culture filtrate from isolates from immunocompetent patients is associated with a significant increase in the hazard of death (HR 10.0; 95CI 5.6-17.9) P< 0.001 sCF-immunocompetent vs naïve.

Figure 4B: Growth of naïve environmental strain nLD2 in media supplemented with sterile culture filtrate from HIV derived VNIa-4 lineage isolates does not result in increased virulence in the *Galleria* model. The naïve LD2 strain was grown in media supplemented with pooled sterile culture filtrate from isolates BK80 or BK224 (VNIa-4 lineage strains derived from the cerebrospinal fluid of HIV infected patients). Infection with the LD2 environmental isolate grown in sCF from isolates of the VNIa-4 lineage did not alter the hazard of death compared with infection with LD2 (HR 0.6; 95CI 0.2, 2.0, P=0.5.

Figure 4C: Growth of naïve environmental strain nLD2 in media supplemented with sterile culture filtrate from the *Cryptococcus neoformans* H99 type strain does not result in increased virulence in the *Galleria* model. H99 was significantly more virulent than naïve DL2 (HR 28.7 (14-60.4) and P<0.001 for H99 vs LD2) but there was no change in the hazard of death for *Galleria* between infection with either the naïve or H99 induced environmental isolate HR 1.3 (0.8-2.2) and P=0.25 for iLD2 vs nLD2 N = 40 larvae per arm.

Figure 4D. The virulence of the LD2 environmental isolate is not increased by growth in media supplemented with sterile culture filtrate derived from previous culture of its naïve state (HR 1.4, 95% CI 0.9-2.2, P=0.2).

720 **5. Figure 5**
721

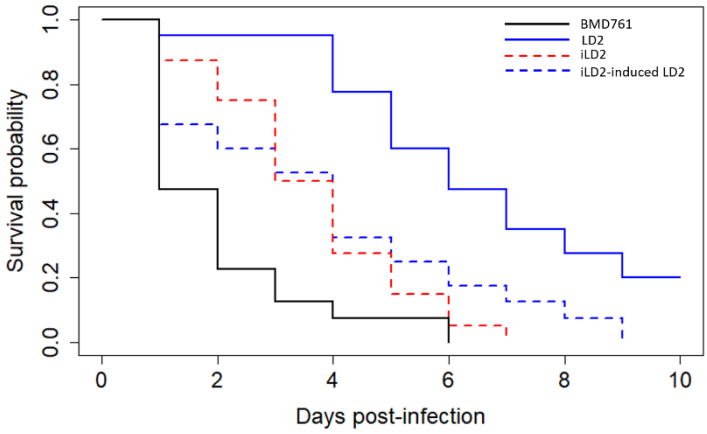

722
723
724 **Figure 5: Survival curves for *Galleria* infected with one of 4 VNIa-5 isolates:** BMD761: isolate from
725 immunocompetent patient; LD2: 'naïve' environmental isolate; induced LD2: naïve LD2 isolate that
726 has been grown with sterile culture filtrate (sCF) from BMD761 (HR 8.2 (4.9-13.8), P<0.001 vs LD2);
727 iLD2-induced LD2: naïve LD2 isolate grown with sCF from iLD2 (HR 2.8 (1.7-4.4), P<0.001 vs LD2).
728 N=40 larvae per arm
729
730

6. Figure 6

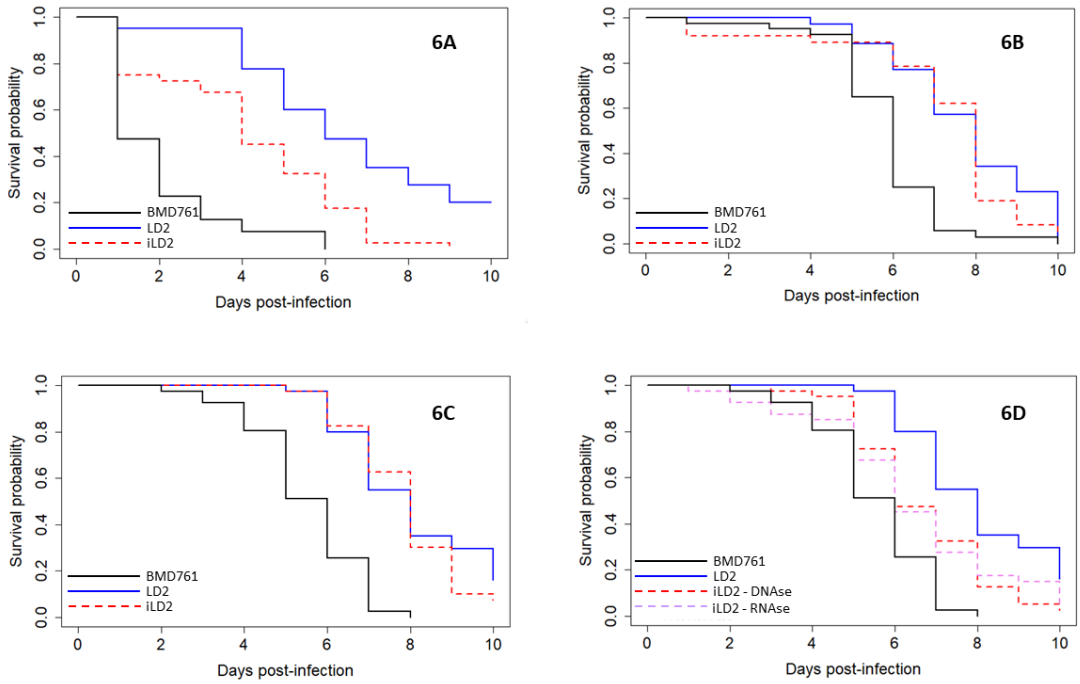

Figure 6: The effects of treating sterile culture filtrate from highly virulent strain BMD761 with either freezing, boiling, protease or nuclease on its ability to induce increased virulence in the naïve environmental strain LD2. Each figure shows survival curves for *Galleria* infected with different *C. neoformans* isolates. BMD761 is the high virulence VNIa-5 lineage isolate derived from an HIV uninfected patient, LD2 is a low virulence VNIa-5 lineage isolate derived from the environment, and induced LD2 is the naïve environmental LD2 isolate following growth in media supplemented with sterile culture filtrate from BMD761.

Figure 6A: The inducing effect of sterile culture filtrate is not affected by freezing at -20C. HR 2.7 95%CI 1.7, 4.5 P<0.001

Figure 6B. Boiling abolishes the induction effect of sterile culture filtrate. HR1.3 95%CI 0.8, 2.01, P=0.3.

Figure 6C: **The inducing effect of sterile culture filtrate is abolished by treatment with proteinase**. HR1.2, 95CI 0.8, 2.0, P=0.36

Figure 6D. **Treatment with DNAse or RNase has no effect on the induction effect of sterile culture filtrate.** DNAse HR 2.1, 95CI 1.3, 3.4, P=0.002; RNAse HR 2.0, 95CI 1.2, 3.4, P=0.004.

N = 30 *Galleria* per arm for all experiments.

7. Figure 7

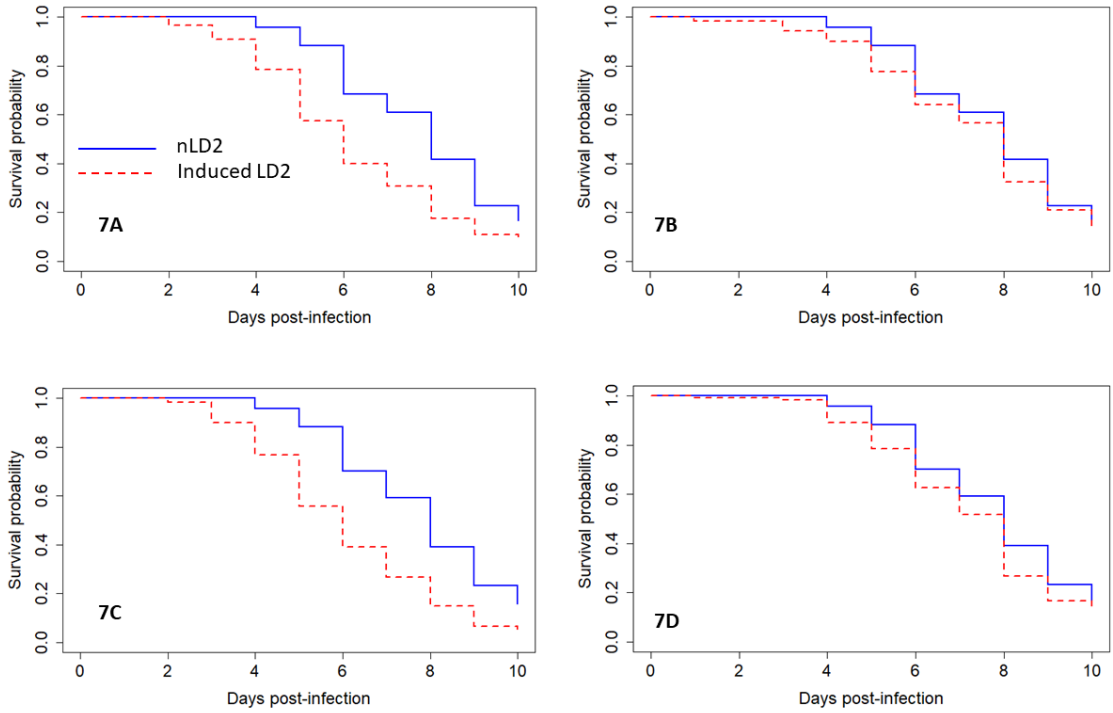

Figure 7: The effect of ultracentrifugation of sterile culture filtrate on induction of virulence in naïve environmental isolate nLD2.

Sterile culture filtrate, derived either from highly virulent isolate BMD761, or from LD2 strain following virulence induction with sterile culture filtrate from BMD761, underwent an extracellular vesicle (EV) isolation protocol to produce a putatively EV containing pellet, and an EV-free supernatant. These fractions were then added to broth culture of naïve LD2 isolate, and the relative virulence of naïve LD2 was compared with subsequent 'induced LD2' (iLD2). Experiments were done in triplicate, N=80 *Galleria* per arm. Summated data shown.

Figure 7A: Growth of LD2 in media supplemented with ultracentrifugation pellet derived from BMD761 sterile culture filtrate (sCF). Induction of increased virulence is seen, HR 1.8, 95CI 1.4, 2.4; P<0.001.

Figure 7B: Growth of LD2 in media supplemented with ultracentrifugation supernatant derived from BMD761 sCF. No induction of virulence in LD2 is seen, HR 1.2, 95CI 0.8, 1.5; P=0.3.

Figure 7C: Growth of LD2 in media supplemented with ultracentrifugation pellet derived from sCF from LD2 that has previously been induced with BMD761 sCF. Induction of increased virulence is seen, HR 2.1, 95CI 1.6, 2.7; P<0.001.

Figure 7D: Growth of LD2 in media supplemented with ultracentrifugation supernatant derived from sCF from LD2 that has previously been induced with BMD761. No induction of increased virulence is seen, HR 1.2, 95CI 0.9, 1.6; P=0.1.

In all panels the solid blue line represents *Galleria* infected with naïve LD2 (nLD2) and the red dashed line represents *Galleria* infected with the 'induced' LD2 (iLD2), i.e. the environmental isolate following growth in media supplemented with either pellet or supernatant.

774 **8. Figure 8**

775

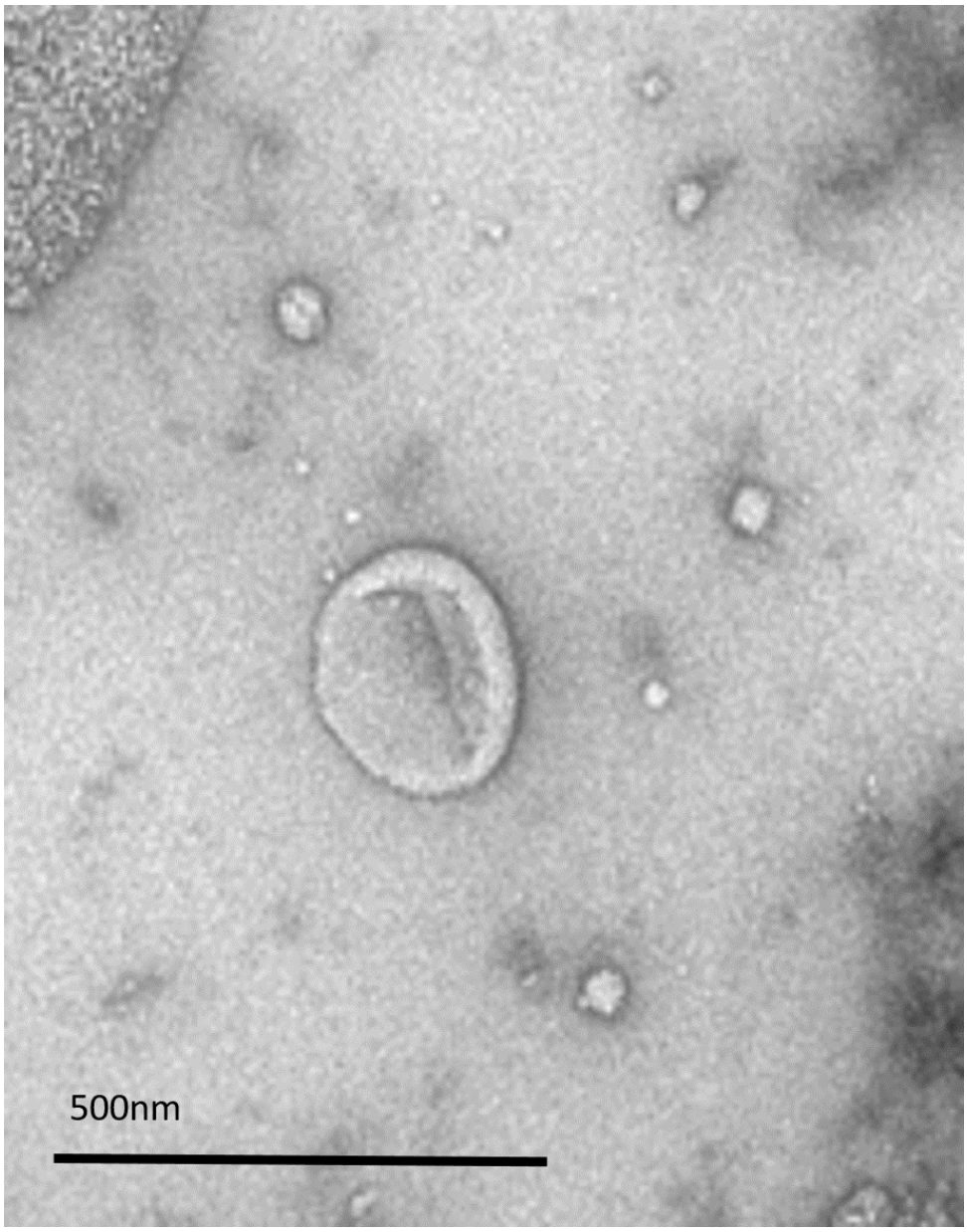

776

777

778

779 **Figure 8: Transmission electron micrograph showing example of extracellular vesicle in**

780 **ultracentrifugation pellet of BMD761.**

781

782 **Figure 9**

783

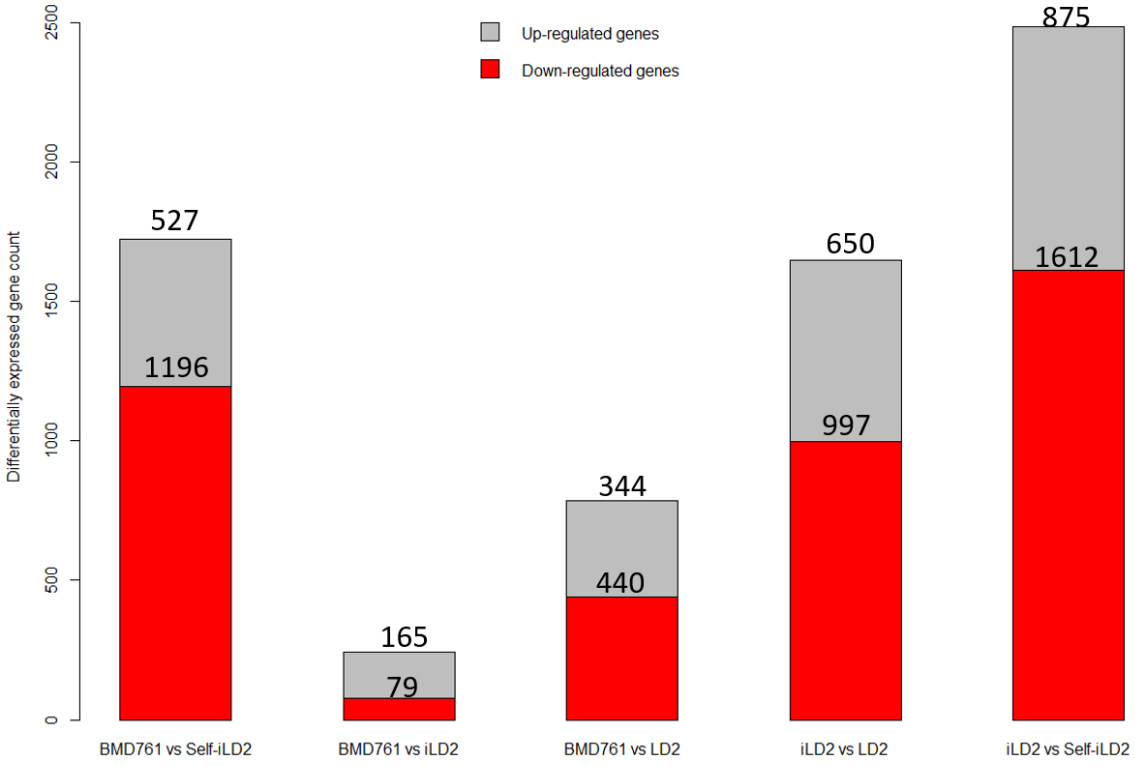

784 **Figure 9: The number of differentially expressed genes between different samples**
785 **(outliers removed).** Genes were counted as differentially expressed if they had a
786 Benjamani-Hochberg adjusted P-value of <0.05, and log2 fold change ≥1 and ≤-1.
787
788
789

References

1. Hagen F, Khayhan K, Theelen B, Kolecka A, Polacheck I, Sionov E, Falk R, Parnmen S, Lumbsch HT, Boekhout T. Recognition of seven species in the Cryptococcus gattii/Cryptococcus neoformans species complex. *Fungal Genet Biol.* 2015;78:16-48.
2. Casadevall A, Perfect JR. *Cryptococcus neoformans.* 1 ed. Washington: American Society for Microbiology Press; 1998.
3. Bartlett KH, Kidd SE, Kronstad JW. The Emergence of Cryptococcus gattii in British Columbia and the Pacific Northwest. *Curr Infect Dis Rep.* 2008;10(1):58-65.
4. Rajasingham R, Smith RM, Park BJ, Jarvis JN, Govender NP, Chiller TM, Denning DW, Loyse A, Boulware DR. Global burden of disease of HIV-associated cryptococcal meningitis: an updated analysis. *Lancet Infect Dis.* 2017;17(8):873-881.
5. Ashton PM, Thanh LT, Trieu PH, Van Anh D, Trinh NM, Beardsley J, Kibengo F, Chierakul W, Dance DAB, Rattanavong S, Davong V, Hung LQ, Chau NVV, Tung NLN, Chan AK, Thwaites GE, Lalloo DG, Anscombe C, Nhat LTH, Perfect J, Dougan G, Baker S, Harris S, Day JN. Three phylogenetic groups have driven the recent population expansion of Cryptococcus neoformans. *Nat Commun.* 2019;10(1):2035.
6. Day JN, Qihui S, Thanh LT, Trieu PH, Van AD, Thu NH, Chau TTH, Lan NPH, Chau NVV, Ashton PM, Thwaites GE, Boni MF, Wolbers M, Nagarajan N, Tan PBO, Baker S. Comparative genomics of Cryptococcus neoformans var. grubii associated with meningitis in HIV infected and uninfected patients in Vietnam. *PLoS Negl Trop Dis.* 2017;11(6):e0005628.
7. Thanh LT, Phan TH, Rattanavong S, Nguyen TM, Duong AV, Dacon C, Hoang TN, Nguyen LPH, Tran CTH, Davong V, Nguyen CVV, Thwaites GE, Boni MF, Dance D,

814 Ashton PM, Day JN. Multilocus sequence typing of Cryptococcus neoformans var.
815 grubii from Laos in a regional and global context. *Med Mycol.* 2018.
816 8. Chen J, Varma A, Diaz MR, Litvintseva AP, Wollenberg KK, Kwon-Chung KJ.
817 Cryptococcus neoformans strains and infection in apparently immunocompetent
818 patients, China. *Emerg Infect Dis.* 2008;14(5):755-762.
819 9. Chen YC, Chang SC, Shih CC, Hung CC, Luhbd KT, Pan YS, Hsieh WC. Clinical features
820 and in vitro susceptibilities of two varieties of Cryptococcus neoformans in Taiwan.
821 *Diagn Microbiol Infect Dis.* 2000;36(3):175-183.
822 10. Choi YH, Ngamskulrungroj P, Varma A, Sionov E, Hwang SM, Carriconde F, Meyer W,
823 Litvintseva AP, Lee WG, Shin JH, Kim EC, Lee KW, Choi TY, Lee YS, Kwon-Chung KJ.
824 Prevalence of the VNIc genotype of Cryptococcus neoformans in non-HIV-associated
825 cryptococcosis in the Republic of Korea. *FEMS Yeast Res.* 2010;10(6):769-778.
826 11. Feng X, Yao Z, Ren D, Liao W, Wu J. Genotype and mating type analysis of
827 Cryptococcus neoformans and Cryptococcus gattii isolates from China that mainly
828 originated from non-HIV-infected patients. *FEMS Yeast Res.* 2008.
829 12. Chau TT, Mai NH, Phu NH, Nghia HD, Chuong LV, Sinh DX, Duong VA, Diep PT,
830 Campbell JI, Baker S, Hien TT, Lalloo DG, Farrar JJ, Day JN. A prospective descriptive
831 study of cryptococcal meningitis in HIV uninfected patients in Vietnam - high
832 prevalence of Cryptococcus neoformans var grubii in the absence of underlying
833 disease. *BMC Infect Dis.* 2010;10:199.
834 13. Day JN, Hoang TN, Duong AV, Hong CT, Diep PT, Campbell JI, Sieu TP, Hien TT, Bui T,
835 Boni MF, Lalloo DG, Carter D, Baker S, Farrar JJ. Most Cases of Cryptococcal
836 Meningitis in HIV-Uninfected Patients in Vietnam Are Due to a Distinct Amplified

Fragment Length Polymorphism-Defined Cluster of Cryptococcus neoformans var. grubii VN1. *J Clin Microbiol.* 2011;49(2):658-664.

14. Bielska E, Sisquella MA, Aldeieg M, Birch C, O'Donoghue EJ, May RC. Pathogen-derived extracellular vesicles mediate virulence in the fatal human pathogen Cryptococcus gattii. *Nat Commun.* 2018;9(1):1556.

15. Sayers S, Li L, Ong E, Deng S, Fu G, Lin Y, Yang B, Zhang S, Fa Z, Zhao B, Xiang Z, Li Y, Zhao XM, Olszewski MA, Chen L, He Y. Victors: a web-based knowledge base of virulence factors in human and animal pathogens. *Nucleic Acids Res.* 2019;47(D1):D693-D700.

16. Wolf JM, Rivera J, Casadevall A. Serum albumin disrupts Cryptococcus neoformans and Bacillus anthracis extracellular vesicles. *Cell Microbiol.* 2012;14(5):762-773.

17. Edskes HK, Khamar HJ, Winchester CL, Greenler AJ, Zhou A, McGlinchey RP, Gorkovskiy A, Wickner RB. Sporadic distribution of prion-forming ability of Sup35p from yeasts and fungi. *Genetics.* 2014;198(2):605-616.

18. Jurka J, Kapitonov VV, Pavlicek A, Klonowski P, Kohany O, Walichiewicz J. Repbase Update, a database of eukaryotic repetitive elements. *Cytogenet Genome Res.* 2005;110(1-4):462-467.

19. Albuquerque PC, Nakayasu ES, Rodrigues ML, Frases S, Casadevall A, Zancope-Oliveira RM, Almeida IC, Nosanchuk JD. Vesicular transport in Histoplasma capsulatum: an effective mechanism for trans-cell wall transfer of proteins and lipids in ascomycetes. *Cell Microbiol.* 2008;10(8):1695-1710.

20. Rodrigues ML, Nakayasu ES, Oliveira DL, Nimrichter L, Nosanchuk JD, Almeida IC, Casadevall A. Extracellular vesicles produced by Cryptococcus neoformans contain protein components associated with virulence. *Eukaryot Cell.* 2008;7(1):58-67.

861 21. Rodrigues ML, Nimrichter L, Oliveira DL, Frases S, Miranda K, Zaragoza O, Alvarez M,
862 Nakouzi A, Feldmesser M, Casadevall A. Vesicular polysaccharide export in
863 Cryptococcus neoformans is a eukaryotic solution to the problem of fungal trans-cell
864 wall transport. *Eukaryot Cell.* 2007;6(1):48-59.
865 22. Rodrigues ML, Nimrichter L, Oliveira DL, Nosanchuk JD, Casadevall A. Vesicular Trans-
866 Cell Wall Transport in Fungi: A Mechanism for the Delivery of Virulence-Associated
867 Macromolecules? *Lipid Insights.* 2008;2:27-40.
868 23. Rodrigues ML, Casadevall A. A two-way road: novel roles for fungal extracellular
869 vesicles. *Mol Microbiol.* 2018;110(1):11-15.
870 24. Ofir-Birin Y, Regev-Rudzki N. Extracellular vesicles in parasite survival. *Science.*
871 2019;363(6429):817-818.
872 25. Konoshenko MY, Lekchnov EA, Vlassov AV, Laktionov PP. Isolation of Extracellular
873 Vesicles: General Methodologies and Latest Trends. *Biomed Res Int.*
874 2018;2018:8545347.
875 26. Casadevall A. Amoeba provide insight into the origin of virulence in pathogenic fungi.
876 *Adv Exp Med Biol.* 2012;710:1-10.
877 27. Casadevall A, Fu MS, Guimaraes AJ, Albuquerque P. The 'Amoeboid Predator-Fungal
878 Animal Virulence' Hypothesis. *J Fungi (Basel).* 2019;5(1).
879 28. Coelho C, Bocca AL, Casadevall A. The tools for virulence of Cryptococcus
880 neoformans. *Adv Appl Microbiol.* 2014;87:1-41.
881 29. Derengowski Lda S, Paes HC, Albuquerque P, Tavares AH, Fernandes L, Silva-Pereira I,
882 Casadevall A. The transcriptional response of Cryptococcus neoformans to ingestion
883 by Acanthamoeba castellanii and macrophages provides insights into the
884 evolutionary adaptation to the mammalian host. *Eukaryot Cell.* 2013;12(5):761-774.

30. Nguyen VTT, Phan HT, Kato M, Nguyen QT, Le Ai KA, Vo SH, Thanh DC, Baggaley RC, Johnson CC. Community-led HIV testing services including HIV self-testing and assisted partner notification services in Vietnam: lessons from a pilot study in a concentrated epidemic setting. *J Int AIDS Soc.* 2019;22 Suppl 3:e25301.

31. Beardsley J, Wolbers M, Kibengo FM, Ggayi AB, Kamali A, Cuc NT, Binh TQ, Chau NV, Farrar J, Merson L, Phuong L, Thwaites G, Van Kinh N, Thuy PT, Chierakul W, Siriboon S, Thiansukhon E, Onsanit S, Supphamongkholchaikul W, Chan AK, Heyderman R, Mwinjiwa E, van Oosterhout JJ, Imran D, Basri H, Mayxay M, Dance D, Phimmasone P, Rattanavong S, Lalloo DG, Day JN, CryptoDex I. Adjunctive Dexamethasone in HIV-Associated Cryptococcal Meningitis. *N Engl J Med.* 2016;374(6):542-554.

32. Day JN, Chau TT, Wolbers M, Mai PP, Dung NT, Mai NH, Phu NH, Nghia HD, Phong ND, Thai CQ, Thai le H, Chuong LV, Sinh DX, Duong VA, Hoang TN, Diep PT, Campbell JI, Sieu TP, Baker SG, Chau NV, Hien TT, Lalloo DG, Farrar JJ. Combination antifungal therapy for cryptococcal meningitis. *N Engl J Med.* 2013;368(14):1291-1302.

33. Lee A, Toffaletti DL, Tenor J, Soderblom EJ, Thompson JW, Moseley MA, Price M, Perfect JR. Survival defects of Cryptococcus neoformans mutants exposed to human cerebrospinal fluid result in attenuated virulence in an experimental model of meningitis. *Infect Immun.* 2010;78(10):4213-4225.

34. Zaragoza O, Casadevall A. Experimental modulation of capsule size in Cryptococcus neoformans. *Biol Proced Online.* 2004;6:10-15.

35. Salas SD, Bennett JE, Kwon-Chung KJ, Perfect JR, Williamson PR. Effect of the laccase gene CNLAC1, on virulence of Cryptococcus neoformans. *J Exp Med.* 1996;184(2):377-386.

908 36. Eisenman HC, Mues M, Weber SE, Frases S, Chaskes S, Gerfen G, Casadevall A.
909 Cryptococcus neoformans laccase catalyses melanin synthesis from both D- and L-
910 DOPA. *Microbiology.* 2007;153(Pt 12):3954-3962.
911 37. Chen SC, Muller M, Zhou JZ, Wright LC, Sorrell TC. Phospholipase activity in
912 Cryptococcus neoformans: a new virulence factor? *J Infect Dis.* 1997;175(2):414-420.
913 38. Liao Y, Smyth GK, Shi W. featureCounts: an efficient general purpose program for
914 assigning sequence reads to genomic features. *Bioinformatics.* 2014;30(7):923-930.
915 39. Love MI, Huber W, Anders S. Moderated estimation of fold change and dispersion
916 for RNA-seq data with DESeq2. *Genome Biol.* 2014;15(12):550.
917 40. Love MI, Anders S, Kim V, Huber W. RNA-Seq workflow: gene-level exploratory
918 analysis and differential expression. *F1000Res.* 2015;4:1070.
919